Quiet Direct Simulation (QDS) of Viscous Flow Using the Chapman-Enskog Distribution

M.R. Smith[a], F.-A. Kuo[a], H.M. Cave[b], M.C. Jermy[b] and J.-S. Wu[c]

[a] *National Center for High-performance Computing, HsinChu, Taiwan.*
[b] *Department of Mechanical Engineering, University of Canterbury, Christchurch NZ.*
[c] *Department of Mechanical Engineering, National Chiao Tung University, HsinChu, Taiwan.*

Abstract. Presented here is the QDS method modified to employ an arbitrary governing velocity probability distribution. An algorithm is presented for the computation of QDS particle "blueprints". The method, which employs a known continuous velocity probability distribution function, uses a set of fixed QDS particle "weights", which can be arbitrarily selected. Provided the weights, particle "blueprint" velocities are computed by taking multiple moments around the governing velocity probability distribution function to provide the discrete representation employed by QDS. In particular, we focus on the results obtained when the governing distribution function is the Chapman-Enskog distribution function. Results are shown for several benchmark tests including a one dimensional standing shock wave and a two dimensional lid driven cavity problem. Finally, the performance of QDS when applied to General Purpose computing on Graphics Processing Units (GPGPU) is demonstrated.

Keywords: *Kinetic Theory of Gases, Computational Fluid Dynamics (CFD), Finite Volume Method (FVM)*
PACS: 02.50.Cw, 02.60.Cb, 02.70.Dh, 05.20.Dd, 47.11.Df, 47.10.ad, 47.45.Ab, 47.40.Ki

INTRODUCTION

The Finite Volume Method (FVM) has become one of the key solution methods for problems in Computational Fluid Dynamics (CFD). In any Finite Volume Method, fluxes across cell interfaces are used to evaluate gradient terms in the set of governing Partial Differential Equations (PDEs). A wide variety of methods are available for computation of the fluxes – including a large family of methods based on continuum formulations arising from kinetic theory. Examples of these include works from Pullin [2], Macrossan et al. [3], Xu et al.[4]. The resulting fluxes permit flow, in any single given time step, between cells which share an adjacent interface. This is a consequence of application of the divergence theorem: such methods are herein referred to as "direction decoupled" in reference to the one dimensional reconstruction employed prior to flux computation [5].

An alternate method for simulating gas flow was proposed by Bird [1] in the Direct Simulation Monte Carlo (DSMC). In DSMC, simulation "particles" are used to carry fluxes of mass, momentum and energy from source regions to destination regions, regardless of the underlying computational grid and its alignment. As a continuum equivalent to DSMC, Pullin [2] proposed the Equilibrium Particle Simulation Method (EPSM) where the collision component of DSMC is replaced by forcing particles to assume the Maxwell-Boltzmann particle velocity equilibrium distribution function. Following this, the True Direction Equilibrium Flux Method (TDEFM) was introduced as a continuum, (spatially) first order equivalent of the EPSM method. Comparison against Pullin's Equilibrium Flux Method (EFM), the conventional (direction decoupled) equivalent of TDEFM, showed the effects of direction decoupling to be a function of the local kinetic CFL number. For problems where flows were not aligned with the computational grid, the results obtained by TDEFM have been shown to be superior to direction decoupled equivalents [5].

The transport method employed by DSMC and EPSM were the inspiration behind the Quiet Direct Simulation Monte Carlo method (QDSMC) developed by Albright et al. [6]. In a QDSMC simulation, a small set of simulation particles, with specially assigned thermal velocities, are moved from cell centers to destination regions where their "mass" is linearly interpolated back onto the underlying computational grid. The "particles" used by QDS are constructed from particle "blueprints" and are employed only for continuum flux calculation in a manner similar to Macrossan's Particle Flux Method (PFM) [7]. Following later work by Smith et al. [8], the QDSMC method was

extended to higher order spatial accuracy and renamed as QDS due to its lack of stochastic processes. The QDS method can be shown to be an approximate, computationally efficient equivalent to TDEFM which avoids the evaluation of expensive error and exponential functions. The simple and efficient formulation of QDS also makes it ideal for application to General Purpose computing on Graphics Processing Units (GPGPU). However, the QDS method has only been applied to equilibrium simulation where particle blueprints are computed specifically for the Maxwell Boltzmann equilibrium distribution function.

Presented is an algorithm for the application of QDS to an arbitrary governing probability distribution function. For fixed sets of particle blueprint weights, which can be arbitrarily chosen, the associated set of particle thermal velocities are computed from moments of the governing probability distribution function. Results for a one dimensional standing shock wave problem and a two dimensional lid driven cavity problem are presented. In addition, the parallel implementation of the method using hybrid MPI (for memory distributed system) and CUDA (for graphic processor units, GPUs) will be discussed.

QUIET DIRECT SIMULATION (QDS)

The conventional QDS method, developed by Albright et al. [6] and later by Smith et al. [8], is demonstrated below in brief detail only – further details can be found within the above references. At the heart of the scheme lies the discretization of the governing Maxwell-Boltzmann probability distribution function, given by:

$$f(C) = f_0(C) = \frac{1}{\sqrt{\pi}} \exp\left[-C^2\right] \tag{1}$$

where C is the dimensionless thermal velocity. Albright [6] proposed the continuous distribution function be replaced by a set of simulation particles such that the first moment can be evaluated using Gauss-Hermite integration:

$$\int_{-\infty}^{\infty} \frac{1}{\sqrt{2\pi}} f(\alpha) e^{-\alpha^2/2} d\alpha = \sum_{j=1}^{N} \frac{w_j}{\sqrt{\pi}} f\left(\sqrt{2} q_j\right) \tag{2}$$

where $f(\alpha) = 1$, w_j is the (statistical) particle weighting corresponding to the jth weight of the quadrature and q_j is the characteristic dimensionless thermal speed corresponding to the jth abscissa of the quadrature. It can be shown that the numerical evaluation of this integral is analytically exact and no approximation is entered into. The particle properties w_j and q_j represent the "blueprint" which is used in all cells. Prior to computation of the actual fluxes, particles located within cell i are computed with the properties:

$$p_{M,j} = (\rho_i V_i) \frac{w_j}{\sqrt{\pi}} \qquad p_{V,j} = u_i + \sqrt{2RT_i} q_j \qquad p_{E,j} = p_{M,j} \left(\frac{p_{v,j}^2}{2} + \varepsilon_{in} \right) \tag{3}$$

where subscripts M, V, E indicate particle mass, velocity and energy and ε_{in} is the internal energy including un-simulated translational degrees of freedom . Since the particle velocity scales with the local cell conditions, the method is easily applied in situations where large variations in temperature and speed exist within the simulation domain. In first order accurate simulations, each of these particles is placed at the center of cell i and is moved in molecular free flight over time Δt after which the mass, momentum and energy is linearly interpolated onto the underlying grid. Higher order spatial extension relies on a modification of particle properties based on flow gradients – more detail can be found in [8] – which aids in the removal of a significant amount of the numerical dissipation arising from the free flight phase of the simulation.

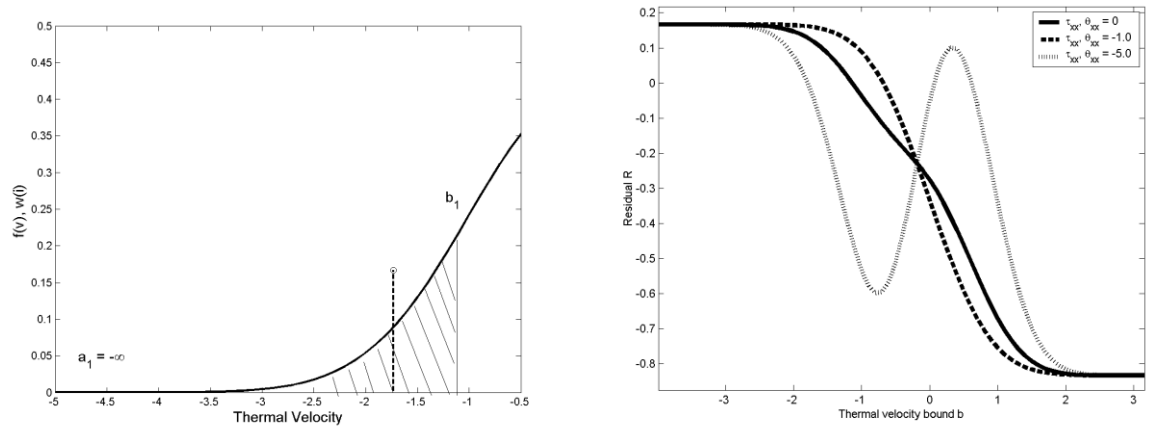

FIGURE 1. [Left] Fraction of mass (shaded region) contained between thermal velocity bounds a = -∞ and b. [Right] The residual function for varying values of shear and heat flux for the left-hand thermal bound a = -∞.

EXTENSION OF QDS TO ARBITRARY DISTRIBUTIONS

The application of the QDS method is shown for an arbitrary distribution function. Following this, the method is tested through application of the Maxwell-Boltzmann distribution function and consequent recovery of the known abscissa taken from Gauss-Hermite quadrature. Finally, the method is applied to the Chapman-Enskog distribution for small deviations from equilibrium. Figure 1 shows the left-most region of a one dimensional distribution function bounded by thermal velocities a_1 and b_1. The fraction contained within this region is given by the weight w_1. In general, the relationship between the fraction w_i contained by bounding thermal velocities a_i and b_i is:

$$\int_{ai}^{bi} f(C)dC = \frac{w_i}{\sqrt{\pi}} \tag{4}$$

Beginning with the left-most region of the distribution function, the left-most thermal velocity bound is known ($a_1 = -\infty$). Thus, with any known fraction (wi), the remaining thermal velocity bound can be computed. Following this, the intial guess for the corresponding abscissa can be computed by taking the mean particle velocity in the region:

$$q_i = \left(\frac{\int_{ai}^{bi} C \cdot f(C)dC}{\int_{ai}^{bi} f(C)dC} \right) = \left(\frac{\sqrt{\pi}}{w_i} \right) \int_{ai}^{bi} C \cdot f(C)dC \tag{5}$$

However, this does not guarantee the energy contained within the resulting simulation particles will equate that of the governing distribution function – so, following calculation of all initial estimates for thermal abscissa, the N abscissa must be further scaled to ensure energy is conserved:

$$\varepsilon = \int_{-\infty}^{\infty} \left(\frac{1}{2} C^2 \right) f(C)dC \qquad \chi = \frac{\varepsilon}{\sum_{i=0}^{N} \frac{w_i}{\sqrt{\pi}} \frac{q_i^{\,2}}{2}} \qquad q = \sqrt{\chi}\left[q_1, q_2 \ldots q_N\right] \tag{6}$$

Verification: Application to the Maxwell-Boltzmann Distribution

Verification of the general algorithm presented is shown for a 3 particle QDS system with standard weights w = $\pi^{1/2}$[1/6, 2/3, 1/6]. The fraction between thermal velocity bounds is given by the general expression:

$$\int_{ai}^{bi} f(C)dC = \frac{W_i}{\sqrt{\pi}} = \frac{1}{2}\left[-erf(a_i) + erf(b_i)\right] \tag{7}$$

Starting with the first particle and known bound a_1, for example, the unknown bound b_1 is computed as $b_1=a_2$= -0.68407. The remaining bounds are computed step-by-step until all are known, providing the result a = [-∞, -0.68407, 0.68407] and b = [-0.68407, 0.68407, ∞]. Following this, the prototype mean thermal velocities are computed by:

$$q_i = \left(\frac{\int_{ai}^{bi} C \cdot f(C)dC}{\int_{ai}^{bi} f(C)dC} \right) = \frac{\left(\exp\left(-a_i^{\,2}\right) - \exp\left(-b_i^{\,2}\right)\right)}{2W_i} \tag{8}$$

which results in the vector of prototype velocities q = [-1.06, 0, 1.06]. However, a quick investigation of these results reveals the total energy to be 0.1873, which is less than the ε = 0.25 predicted by theory. The correction factor is therefore χ=0.25/0.1873=1.3350. Finally, the prototype velocities are scaled to $q = (1.3350)^{1/2}$q, proving the final particle blueprint velocities of q = [-1.2247, 0, 1.2247]. These are the exact abscissa provided by Gauss-Hermite quadrature.

Application to the Chapman Enskog Distribution

The full 3D form of the Chapman-Enskog distribution is given by [9]:

$$f(C_x, C_y, C_z) = f_0(C_x) f_0(C_y) f_0(C_z) \Gamma(C_x, C_y, C_z) \tag{9}$$

where the subscripts (x,y,z) indicate translational degree of freedom and:

$$\begin{aligned} \Gamma(C_x, C_y, C_z) &= 1 + \left(\theta_x C_x + \theta_y C_y + \theta_z C_z\right)\left(\frac{2}{5}\left(C_x^2 + C_y^2 + C_z^2\right) - 1\right) \\ &- 2\left(\tau_{xy} C_x C_y + \tau_{xz} C_x C_z + \tau_{yz} C_y C_z\right) - \tau_{xx}\left(C_x^2 - C_z^2\right) - \tau_{yy}\left(C_y^2 - C_z^2\right) \end{aligned} \tag{10}$$

where τ and θ are shear and heat stress tensors respectively. Integrating around all possible y and z values of thermal velocity provides the one dimensional representation:

$$\begin{aligned} \Gamma(C_x) &= \int_{-\infty}^{\infty}\int_{-\infty}^{\infty} f(C_x, C_y, C_z) dC_z dC_y \\ &= 1 + \theta_x C_x\left(\frac{5}{2} C_x^2 - 1\right) - C_x^2 \tau_{xx} + \frac{2}{5}\theta_x C + \frac{1}{2}\tau_{xx} \end{aligned} \tag{11}$$

The fraction contained within an arbitrary set of bounding thermal velocities is given by:

$$\left(\int_a^b f_0(C_x)\Gamma(C_x)dC_x\right)_i = \frac{W_i}{\sqrt{\pi}} = \left[\frac{\exp\left(-C_x^2\right)}{10\sqrt{\pi}}\left(-2\theta_x C_x^2 + 5\tau_{xx} C_x + \theta_x\right) + \frac{1}{2}\operatorname{erf}(C_x)\right]_{a_i}^{b_i} \tag{12}$$

TABLE (I): Application of QDS to GPGPU across varying numbers of GPU 1060 devices for a two dimensional benchmark problem with 4 million cells.

	X4572 1 CPU	C1060 (x1)	C1060 (x 2)	C1060 (x4)	C1060 (x8)	C1060 (x16)	C1060 (x32)
Speedup Ratio	1	33.3	65.6	124.0	236.8	413.0	623.9
Theoretical Speedup	N/A	1	2	4	8	16	32
Reported Speedup	N/A	1	1.97	3.73	7.12	12.41	18.75
Efficiency	N/A	N/A	98.5%	93.2%	89%	77.6%	58.5%

This presents a dilema – for any known left-hand bound a and weight w, the solution for b is non-linear and an iterative approach must be employed. The residual function to be solved is:

$$R_i = \frac{W_i}{\sqrt{\pi}} - \frac{\exp\left(-b_i^{\,2}\right)}{10\sqrt{\pi}}\left(-2\theta_x b_i^{\,2} + 5\tau_{xx} b_i + \theta_x\right) + \frac{\exp\left(-a_i^{\,2}\right)}{10\sqrt{\pi}}\left(-2\theta_x a_i^{\,2} + 5\tau_{xx} a_i + \theta_x\right) - \frac{1}{2}\left[\operatorname{erf}\left(b_i\right) - \operatorname{erf}\left(a_i\right)\right] \tag{13}$$

This is also shown in Figure 1 for the 3 particle QDS case with weight ($w/\pi^{1/2}$) = 1/6 and left-hand thermal velocity bound a = -∞ for varying values of normalized heat and shear stress. For very large deviations from equilibrium, the residual function has multiple roots. – however, these are non-sensical in that the Chapman-Enskog distribution is only valid for small deviations from equilbrium. Gradients of the residual in regions far from the solution are almost zero, so gradient-based iterative methods are not applicable – a simple bisection method is sufficient in most situations. Following this, the prototype abscissa are computed:

$$q_i = \frac{\sqrt{\pi}}{W_i}\left[\frac{\exp\left(-C_x^2\right)}{10\sqrt{\pi}}\left(-5 + \frac{5}{2}\tau_{xx}\left(1 + 2C_x^2\right) - 2\theta_x C_x^3\right)\right]_{a_i}^{b_i} \tag{14}$$

Finally, the prototype thermal velocities (abscissa) are scaled to ensure energy is conserved. Care must be taken since the Chapman-Enskog distribution is anisotropic and energy distribution is a function of shear stresses. The scaling parameter can be shown to be:

$$\chi = \frac{1 - \tau_{xx}}{4\sum_{i=0}^{N} \frac{w_i}{\sqrt{\pi}} \frac{q_i^{\,2}}{2}} \tag{15}$$

The computational efficiency behind process described can be improved through preparing (for any fixed number of QDS particles) a table or polynomial expressions for blueprint abscissa as a function of heat and shear stress tensors. For briefity, this is ommitted from this investigation.

RESULTS

Parallel Performance using hybrid GPUMPI

The performance of QDS applied to General Purpose-programming of Graphics Processing Units (GPGPU) is shown in Table I. The highly local nature of the QDS scheme, together with efficient use of texture memory present on the Nvidia Tesla C1060 GPU device, allows high levels of speedup with a maximum performance (speedup) of 623 times when compared to a single core of an Intel X5472 Xeon processor for a two dimension shock bubble interaction problem [10].

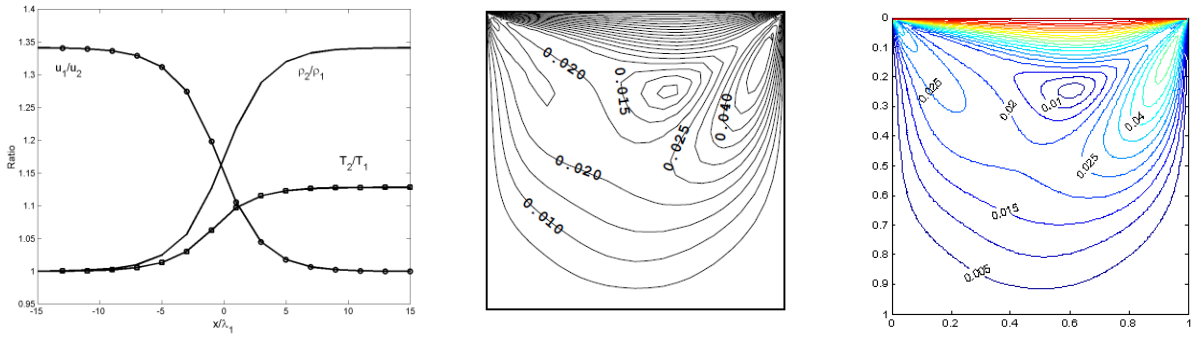

FIGURE 2. [Left] Internal structure of a 1D shock computed using CE-QDS for M_s = 1.2. [Right] Mach number contours for the lid driven cavity problem (Re = 100). [Center] 8th order accurate WENO result [Right] 2nd order CE-QDS results.

1D Shock Wave Internal Structure

As a preliminary test the Chapman-Enskog distribution application to the QDS method has been applied to the solution of the Navier-Stokes equations for one dimensional flow through a plane normal shock wave. The gas is assumed ideal with $\gamma = 1.4$. The viscosity μ is computed by a power-law relationship with w = 0.9 and conductivity computed by $k = 2\mu/(3(\gamma-1))$. The results for a shock wave of strength Ms = 1.2 are shown in Figure 2 with close comparison to results obtained by Macrossan et al. [3].

2D Lid Driven Cavity Problem

The multidimensional extension of the QDS method to viscous flow is applied to a compressible lid driven cavity flow [10]. A box with diffusely reflecting surfaces enclose an ideal gas (γ=1.4) originally at rest. The top surface is given a speed such that the dimensionless properties of the problem are M = 0.001 and Re = 100. The viscosity and conductivity are computed as for the 1D planar shock test. QDS fluxes employ a higher-order construction using a Monotonized Central Difference (MC) limiter to reduce numerical dissipation. Results are shown to be in good comparison with those obtained from Yang et al. [11] as shown in Figure 2.

AKNOWLEDGEMENTS

The first author would like to extend his gratitude to the National Center for High-performance Computing for use of their high-performance GPU cluster. Prof. J.-S. Wu would like to acknowledge the National Science Council (NSC) of Taiwan for the support through research grant NSC-99-2922-I-009-107.

REFERENCES

1. Bird G.A., "Molecular Gas Dynamics and the direct simulation of gas flows", Oxford University Press, 1994.
2. D. Pullin, Direct Simulation Methods for Compressible Inviscid Ideal-gas Flow, *J. Comp. Phys.*, 34[2]: pp. 231-244, 1980.
3. M. N. Macrossan and R.I. Oliver, A Kinetic Theory Solution Method for the Navier-Stokes Equations, *Int. J. Num. Met. Fluids*., 17[3]: pp. 117-193, 1993.
4. K. Xu, A Gas-Kinetic BGK Scheme for the Navier-Stokes Equations and Its Connection with Artificial Dissiaption and Godunov Method, *J. Comp. Phys*., 171[1]: pp. 289-335, 2001.
5. M.R. Smith et al., Effects of Direction Decoupling in Flux Calculation in Euler Solvers, *J. Comp. Phys.*, **227[8]**: pp. 4142-4161, 2008.
6. B.J. Albright et al., Quiet direct simulation of plasmas. *Phys. Plasma*, 9[5]: pp 1898–1904, 2002.
7. M.N. Macrossan et al., Hypersonic flow over a wedge with a Particle Flux Method, in: Proceedings of the 24th International Symposium on Rarefied Gas Dynamics, American Institute of Physics, pp. 650, 2004.
8. M.R. Smith et al, An Improved Quiet Direct Simulation Method for Eulerian Fluids Using a Second-Order Scheme, *J. Comput. Phys*. 228[6]: pp. 2213–2224, 2009.
9. A.L. Garcia and B.J. Alder, Generation of the Chapman-Enskog Distribution, *J. Comp. Phys*, 140[1]:pp. 66-70, 1998.
10. M. Cada and M Torrilhon, Compact third-order limter functions for finite volume methods, *J. Comp. Phys.*, 228[11]:pp. 3118-4145, 2009.
11. Y.-L. Yang and C.-C. Lin, A High Order Pointwise Solution of Compressible Navier-Stokes Equations in Lid-Driven Cavity Flows, *Chung Hua J. Sci. Eng.*, 7[2]: pp. 1-7, 2009.